



INTERNATIONAL JOURNAL OF ENGINEERING SCIENCES & RESEARCH TECHNOLOGY

ANALYSIS ON THE IMPACT OF POWER SYSTEM STABILIZER AND RENEWABLE ENERGY TO SMALL SIGNAL STABILITY OF A POWER SYSTEM

N. M. N Khairu Zaman¹, M. E. Yusoff², H. Hashim³

Electrical Power Engineering, College of Engineering, Universiti Tenaga Nasional,
Jalan IKRAM – UNITEN, 43000 Kajang, Selangor, Malaysia

DOI: 10.5281/zenodo.1401729

ABSTRACT

Renewable energy resources are environmental friendly and provide a lot of benefits to power system network in meeting the increasing demand of electricity. Integration of renewable energy resources to the grid system especially solar photovoltaic that does not have inertia may influence the behavior of power system. This paper analyzes small signal stability in a power system for various scenarios including when the system is subjected to disturbance with and without stabilizer and solar photovoltaic interconnection using PSSE software. The damping ratio and frequency oscillation are evaluated using Prony Method based on Eigenvalue analysis.

KEYWORDS: Small Signal Stability, Eigenvalues, Damping Factor, Accelerating Power, Oscillation Frequency

I. INTRODUCTION

Environmental issues and the depletion of the fuel resources are the motivating force that encouraging researchers to do more research on renewable energy (RE) as alternative energy resources. The demand for solar photovoltaic (PV) has increased faster due to the popularity of solar energy as RE sources [1] - [2]. Total installed capacity of Solar PV under Feed in Tariff (FiT) in Malaysia from 2012 to 2017 is 337.47 MW [3]. The RE resources provide clean energy; based on the literature review, it was found that the connection of RE into the system can improve the grid stability network [1] - [2].

Power system stability is defined as recovery process to regain a state of operating equilibrium after subjected to disturbance. Thus, power system is said to maintain its stability condition if its voltage is within the acceptable limit; the system able to restore the balance between the system generation and load with minimum loss of load, and each generator could maintain the equilibrium between the mechanical torque and the electromagnetic torque [4] - [5]. Therefore, analysis in power system grid network is important as the network needs to maintain its stability after the occurrence of fault.

II. MATERIALS AND METHODS

Small Signal Stability Studies

Power system has many components which interact together and may give rise to the electromechanical mode of oscillation even during normal or contingency condition. If the oscillation continues without sufficient damping, it can lead to system instability. Synchronization of the machine must be maintained for both conditions, before and after disturbance. Two significant components to be monitored when analyzing small signal stability and transient stability are synchronization of rotor angles and rotor speed; however, small signal stability involves small disturbance while transient stability encompasses on large scale [6].

System stability depends very much on the dynamics of generator rotor angles and power angle relationship. The mechanical properties of the generator may also influence the stability of power grid because if any disturbance were to occur, the generator must adjust the angle of the rotor to meet the condition of power transfer [7]. Small signal stability is the capability of the power system to sustain linearization of the system under small disturbance [8], which is frequently related to small disruption such as a slight change in generation or load of the power

system. There are two modes of small signal; oscillatory and non-oscillatory mode. The oscillatory mode is considered as lack of damping torque while non-oscillatory mode is the lack of sufficient of synchronizing torque [5]. For stable state condition, linearization system can be categorized into two different methods. Firstly, the system is stable when it returns to same equilibrium point after disturbance. Second, the system is stable when it returns to new equilibrium point after small fault [6], [9].

Instability causes the rotor angle to increase due to insufficient of synchronizing torque and increase in amplitude of rotor oscillation due to low damping torque. The stability of rotor oscillation consists of several types; local modes, inter-area modes, control modes, and torsional modes. For the local modes, it is more on swinging of units at one generating station. Meanwhile at the inter-area modes, it is more to unsteady on many machines in one part of the system [5]. The characteristic of stability in small signal can be measured through *Lyapunov's first method* that state [1], [8]:

- i) When the eigenvalues have negative real parts, the original system is asymptotically stable.
- ii) When at least one of the eigenvalues has a positive real part, the original system is unstable.
- iii) When the eigenvalues have real parts equal to zero, it is not possible on the basics of the first approximation to say anything in the general.

The stability of the system can be determined by calculating the eigenvalues using Eq. 3.1; in order to prove the system is asymptotically stable or vice versa. A negative eigenvalue shows non-oscillatory mode (not swing) and undergoes decaying process. If one of the eigenvalues has positive real part, the system is said to be unstable. Thus, from the oscillation, the frequency and damping value of the complex eigenvalue can be calculated as in Eq. 3.1 and Eq. 3.2 [6], [8].

$$\lambda = \sigma \pm j\omega \quad (3.1)$$

Where,

λ = eigenvalues; σ = real component; and ω = imaginary component

The frequency of the eigenvalues is given in Eq. 3.2 [6], [8].

$$f = \frac{\omega}{2\pi} \quad (3.2)$$

The damping ratio is given by Eq. 3.3 [6], [8].

$$\xi = \frac{-\sigma}{\sqrt{\sigma^2 + \omega^2}} \quad (3.3)$$

As for complex mode, frequency and damping ratio are measured. The system is unstable if the damping ratio, ξ is negative and the damping margin must be 3% to 5% to ensure good performance [10]. Based on a research paper, the minimum acceptable level of damping is not clearly known [11]; however, following any disturbance the damping ratio of power, angle or voltage oscillation must not be less than 5% based on TNB code of Practice, 2nd Edition [12]. Low frequency oscillation (LFO) is commonly located at a weak connected system whereby the damping is low or negative damping [13]. The LFO occurs because of insufficient damping torque and LFO is categorised into two modes which are local mode with frequency (1-2 Hz) and inter-area mode with frequency (0.1-1 Hz) [13] - [14]. Once damping ratio is calculated, then Eq. 3.4 is used to calculate the amplitude decay [6].


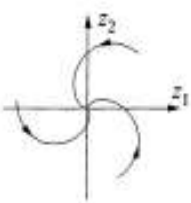
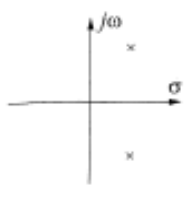
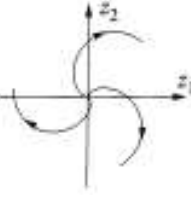
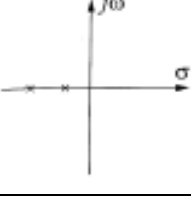
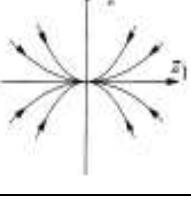
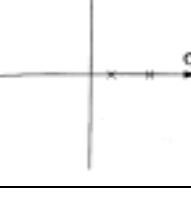
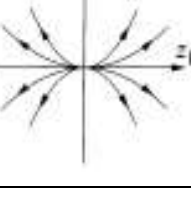
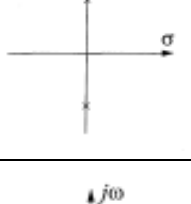
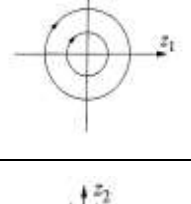
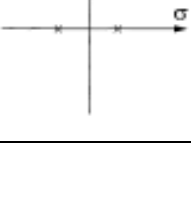
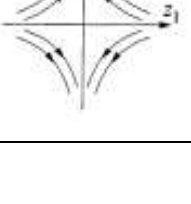
$$\varphi = \frac{1}{\sigma} \quad (3.4)$$

Once eigenvalue is found, eigenvector can be calculated to check another aspect of the system behavior such as mode contribution and shape. Eq. 3.5 gives the right eigenvector for each eigenvalue and mode shape [6].

$$AV_i = \lambda_i V_i \quad (3.5)$$

From the eigenvector expression, the trajectory can be plotted to represent the stability of the system and oscillation mode. Table 1 shows common trajectory illustrated by power system [6].

Table 1: Eigenvalues and Trajectory [8]

Eigenvalues	Trajectory	Type of Singularity
		Stable $(\lambda_{1,2} = -\sigma \pm j\omega)$
		Unstable Focus $(\lambda_{1,2} = \sigma \pm j\omega)$
		Stable Node $(\lambda = -\sigma)$
		Unstable Node $(\lambda = \sigma)$
		Vortex $(\lambda_{1,2} = \pm j\omega)$
		Saddle $(\lambda_{1,2} = \pm\sigma)$

Analysis Technique

Prony Analysis from the modal analysis is used as a method to extend Fourier analysis by directly estimating the frequency, damping, strength and relative phase of modal component. This method decomposes the signal into dominant mode of oscillation, and forms real and imaginary part of eigenvalues, where these are proportional to the mode damping and frequency [11]. The decaying rate of the amplitude of oscillation is best described in terms of damping ratio, ζ [8].

Test System

This research work is using IEEE 14 bus test system with and without stabilizer and solar PV as shown in Figure 1. The test system consists of three gas-fired generators and two coal-fired generators. Three different models of IEEE 14 bus test systems are developed:

- i) IEEE-14 Bus Test System as base case.
- ii) IEEE-14 Bus Test System with stabilizer.
- iii) IEEE-14 Bus Test System with solar photovoltaic.

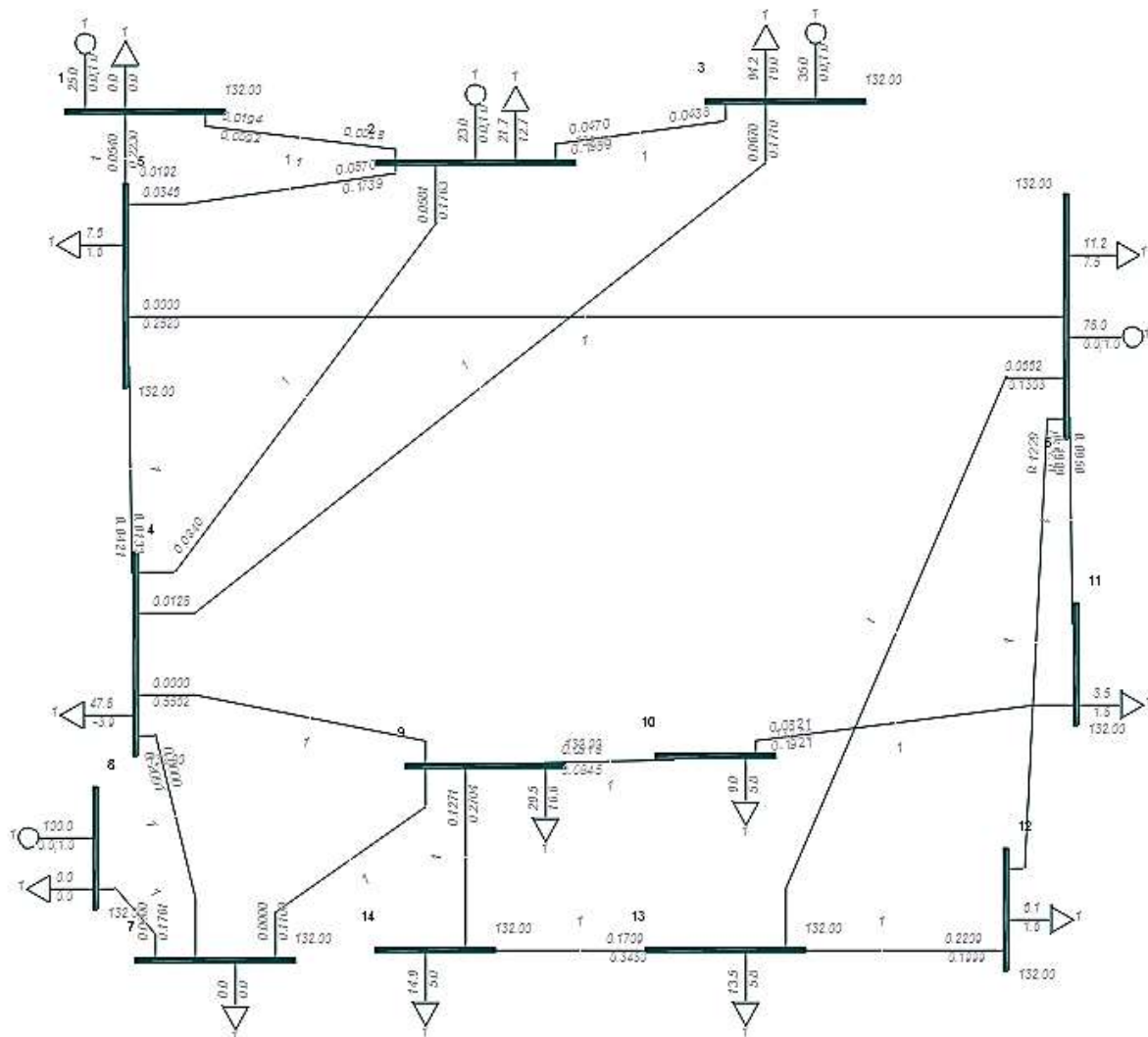


Figure 1: IEEE 14 Bus System

Solar Photovoltaic System Model

The basic structure of developing solar photovoltaic (PV) to simulate the performance of solar PV plant in PSS/E environment is modelled as shown in Figure 2, which demonstrates the connection of single line SPVG.

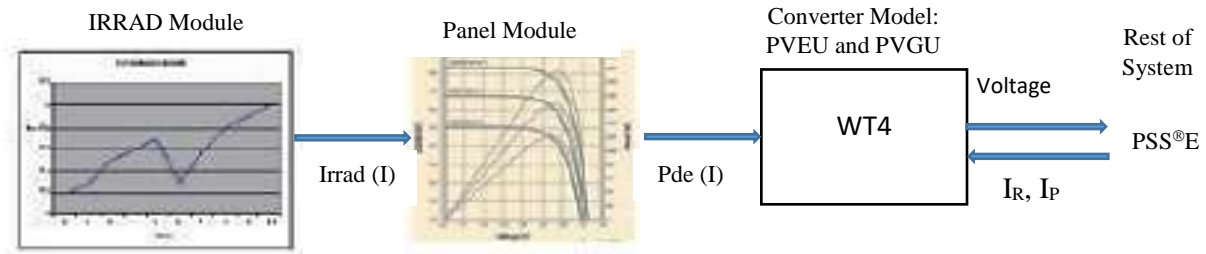


Figure 2: PV Model Connectivity Diagram [15]

The generic type 4 wind model, WT4 is used with added ability to simulate the output changes due to solar irradiation. The PV Generic Wind Model comprises of the following modules [15]:

- i) PVGU - Power Converter/Generator Module
- ii) PVEU - Electrical Control Module
- iii) PANEL - Linearized Model of a Panel's Output Curve
- iv) IRRAD - Linearized Solar Irradiance Profile

N-1 Contingency

The time taken to eliminate a fault at 132kV transmission is 150ms based on TNB code of Practice, 2nd Edition [12]. Figure 3 shows the time line events for both line fault conditions:

- i) Line fault between Bus 2 and Bus 3 when the system is equipped with and without stabilizer and
- ii) Line fault between Bus 3 and Bus 4 when the test system is connected with and without solar PV.

The line fault is applied at 1.0s and followed by tripping the faulted line at a time delay of 150ms. Figure 3 further illustrates the pre-fault, during fault and post fault conditions. The frequency oscillation and damping percentage are obtained after disturbance occurs.

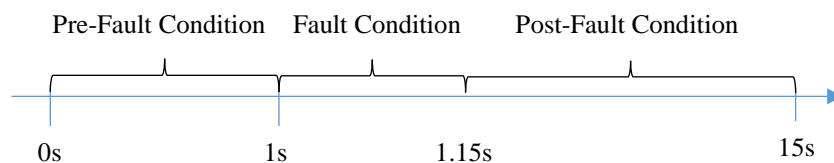


Figure 3: Time Line Event of Dynamic Simulation

Methodology

The flow of the project is illustrated in Figure 4; the project starts with literature review on the related issues. IEEE 14 bus test system is modelled in PSSE environment; the system is stabilized by ensuring that all machines are operating within their capability limits, no voltage violation, and all the branches are not overloaded. The test system is then converted to dynamic state in order to perform fault analysis simulation. A stabilizer is then added at the exciter of the generator for an analysis of fault between Bus 2 and Bus 3, while solar PV is added at Bus 4 which is the generator bus.

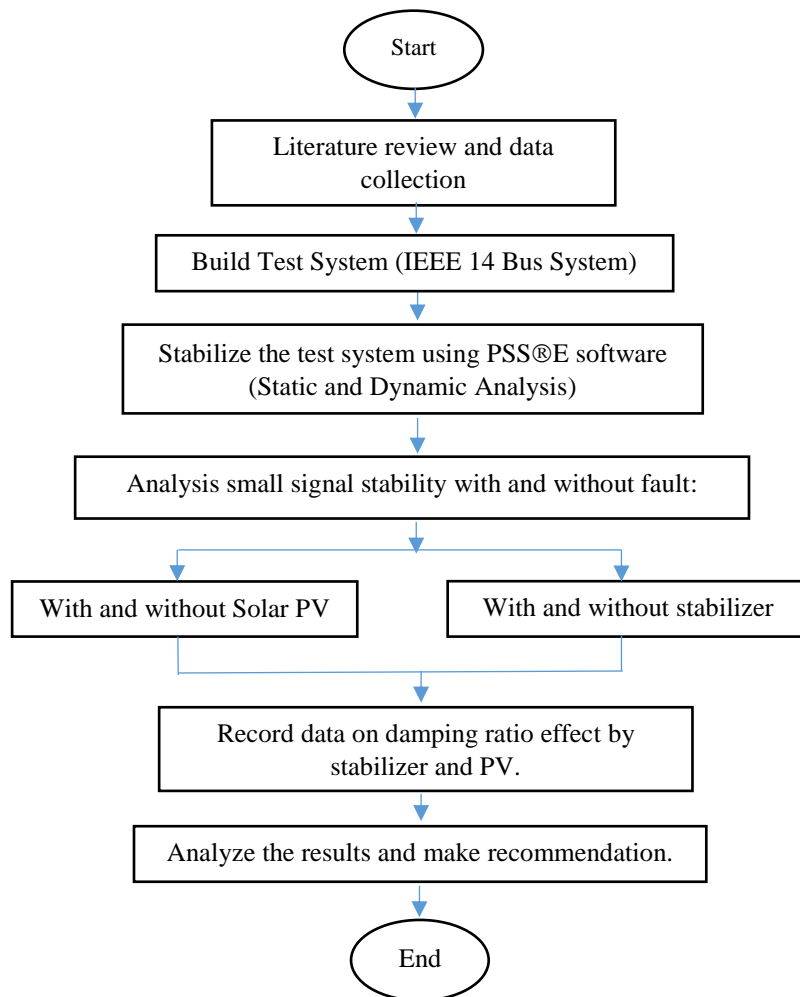


Figure 4: Project Flowchart

III. RESULTS AND DISCUSSION

Based on PSSE dynamic simulation results, the damping ratio, frequency oscillation, the accelerating angle, and eigenvalues of the system are calculated and analyzed for each scenario in order to evaluate the behavior of the system at steady state and fault conditions. Furthermore, the impacts of stabilizer and solar PV to the power system behavior are also examined. Below are the cases of the research work:

- i) Case 1: System at steady state condition.
- ii) Case 2: Line fault between Bus 2 and Bus 3 with and without stabilizer at Bus 3.
- iii) Case 3: Line fault between Bus 3 and Bus 4 with and without solar PV penetration at Bus 4.

Case 1: System at steady state condition

Figure 5 and Table 2 show the rotor angle of generator buses when the system is at stable condition with Generator 1 serves as reference. It is proven that there is no oscillation in rotor angle as they are operating at constant power angle.

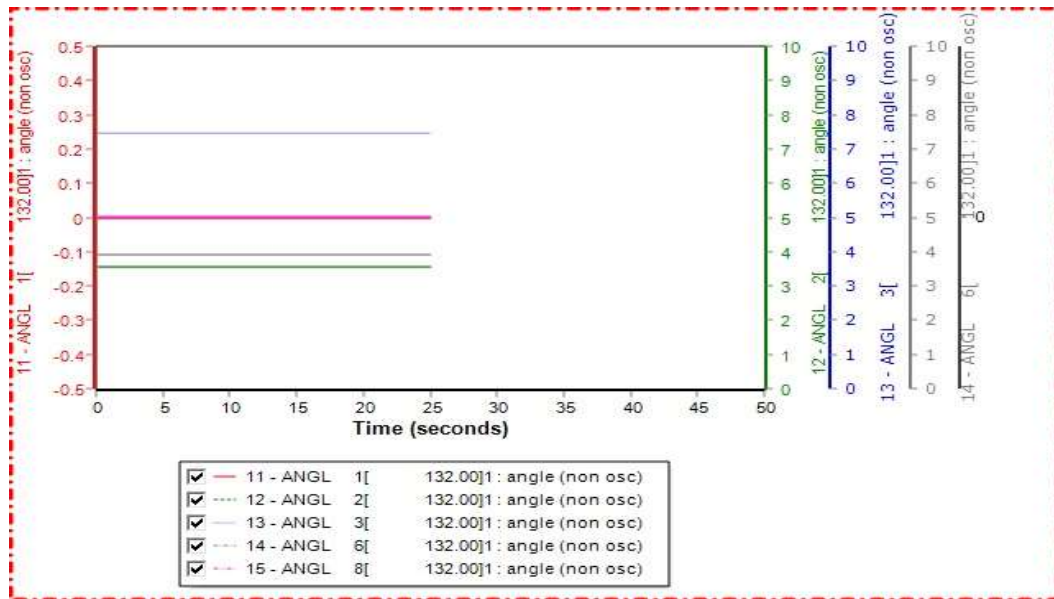


Figure 5: Rotor Angle at Static Condition.

Table 2: Rotor Angle for Case Study 1

Generator Bus Number	Deviation of Rotor Angle from Reference Generator, δ (degree)
1 (Reference Generator)	0
2	-0.14
3	0.25
6	-0.1
8	0

Case 2: Line fault between Bus 2 and Bus 3 with and without stabilizer at Bus 3.

Without stabilizer

Bus 3 is chosen to investigate the damping ratio because a combination of 94.2 MW and 19 MVar load is connected to this bus, which is the largest load in the system. Line fault is applied between Bus 2 and Bus 3 as shown in Figure 6.

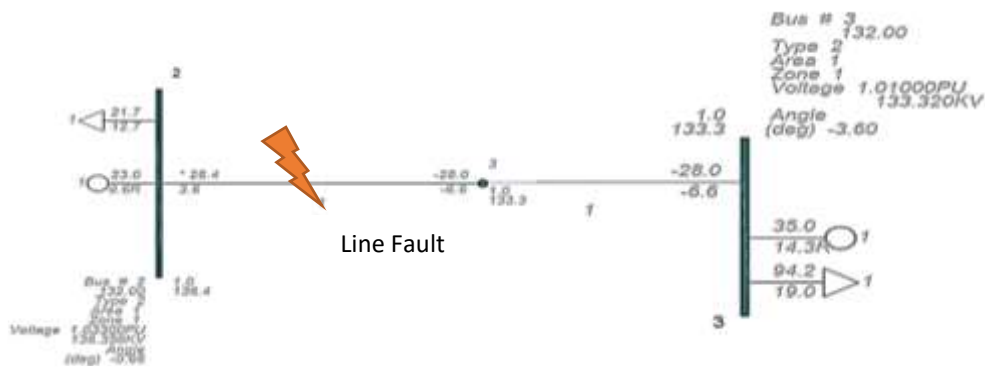


Figure 6: Illustration for Line Connection between Bus 2 and Bus 3

Figure 7 shows the behavior of Generator 3 rotor angle during sub-transient, transient and steady state condition when the line connecting between Bus 2 to Bus 3 experiences fault without stabilizer. The generators are hunting for a new equilibrium point with a settling time of 7 seconds.

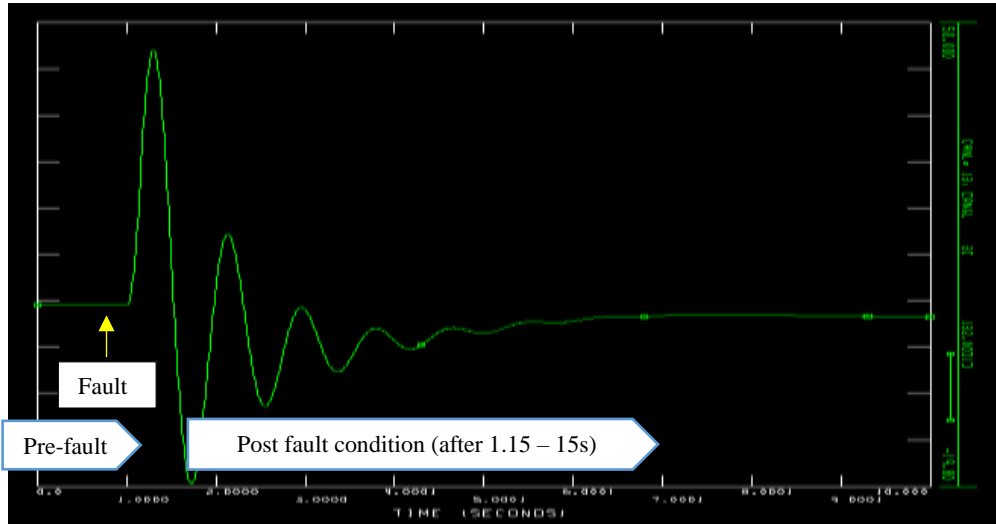


Figure 7: Rotor Angle at Bus 3 without Stabilizer at Bus 3

Based on the results, the eigenvalue can be obtained using Prony Method being generated by PSS[®]E software in PSSPLT. The eigenvalues are used to calculate the damping ratio in order to determine the stability whether the system is underdamped, critically damped and overdamped. If the damping ratio is between 0 and less than 1.0, it is categorized as underdamped; however, if damping ratio is 1.0, the system is considered as critically damped. Nevertheless, if the damping ratio is above 1.0, the system is said to experience overdamped condition [16].

Referring to Table 3, component 1-3, 6-10, and 12-13 have negative damping ratio while only component 4, 5 and 11 have positive damping ratio; hence, majority of the components are negative. Based on the concept, the system is unstable if the damping ratio, ξ is negative. The value of damping ratio is fluctuating as they increase by number of components. All the components of the damping ratio are neither critically damped nor overdamped except for component 4, 5 and 11 which show that the system experiences underdamped.

Table 3: Damping Ratio for Case 2 without Stabilizer

Component	Eigenvalues		Real, σ	Imaginary, ω	Damping ratio, ξ	Frequency, Hz
	Real	Imaginary				
1	0.3576-E04	-	3.57623E-05	0	-1	0
2	2.0706	7.1934	2.071	7.194	-0.277	1.145
3	3.1576	17.9809	3.158	17.981	-0.173	2.862
4	-0.58112	37.9314	-0.581	37.931	0.015	6.037
5	-8.1084	97.1301	-8.108	97.130	0.083	15.459
6	1.0056	61.202	1.006	61.920	-0.016	9.855
7	0.2828	83.6784	0.283	83.678	-0.003	13.318
8	3.8161	47.0328	3.816	47.033	-0.081	7.485
9	4.9112	69.5790	4.911	69.579	-0.070	11.074
10	1.9919	112.7470	1.991	112.747	-0.018	17.944
11	-0.3476	127.9050	-0.348	127.905	0.003	20.357
12	2.5725	145.9810	2.573	145.981	-0.018	23.234
13	11.1248	106.6350	11.125	106.635	-0.104	16.971

• **With Stabilizer at Bus 3**

The line fault is applied between Bus 2 to Bus 3, with stabilizer connected to Bus 3. IEEE type PSS3B stabilizer with dual input is chosen because PSS3B stabilizer has better performance in improving stability [17]. Figure 8 shows the result of rotor angle at Bus 3 when connected with PSS3B stabilizer. The settling time to achieve steady state is 6.7 seconds which is faster compared to the system without stabilizer where with a settling time is 7 seconds. The eigenvalues of the results are tabulated in Table 4.

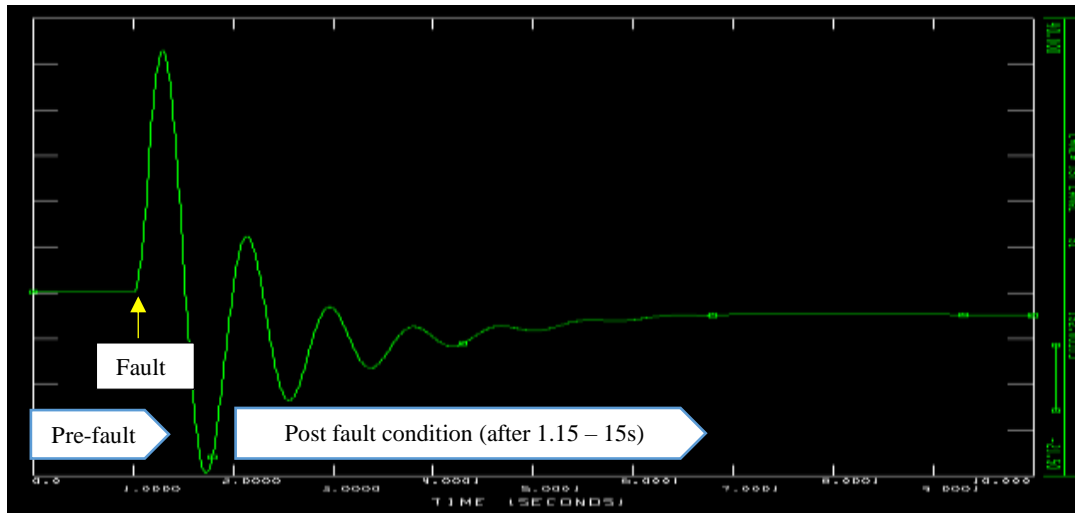


Figure 8: Rotor Angle at Bus 3 with Stabilizer at Bus 3

Table 4: Damping Ratio for Case 2 with PSS3B Stabilizer at Bus 3

Component	Eigenvalues		Real, σ	Imaginary, ω	Damping ratio, ξ	Frequency, Hz
	Real	Imaginary				
1	0.3947E-02	-	0	0	-1	0
2	0.1322	1.2598	0.132	1.260	-0.104	0.201
3	-72.5701	67.3652	-72.570	67.365	0.733	10.722
4	-0.2430	22.6751	-0.243	22.675	0.011	3.609
5	-0.9203	33.9013	-0.920	33.901	0.027	5.396
6	-0.6844	53.5921	-0.684	53.592	0.013	8.529
7	-1.2397	109.8830	-1.240	109.883	0.011	17.488
8	-1.2530	90.1823	-1.253	90.182	0.014	14.353
9	1.5889	61.9314	1.589	61.931	-0.026	9.857
10	-1.0124	146.2350	-1.012	146.235	0.007	23.274
11	0.6478	79.6209	0.648	79.621	-0.008	12.672
12	1.0364	120.3400	1.036	120.340	-0.009	19.153
13	2.0465	137.7240	2.046	137.724	-0.015	21.919

Based on Table 4, the component 1-2, 9, and 11-13 have negative damping ratio while component 3-8 and 10 have positive damping ratio. Hence when stabilizer is connected to Bus 3, majority of the components have positive damping ratio. Furthermore, with stabilizer, the values of damping ratio increase compared to without stabilizer; for example, at component 2, the damping ratio has increased from -0.277 to -0.104. Another example, the damping ratio at component 3 has improved from 17.3% to 73.3%; thus, this shows that the stability of the system improves as the damping ratio increases [1] - [2].

Figure 9 shows the excursion of the angle deviation at Bus 3 with and without stabilizer; the angle deviation is reduced with stabilizer connected at Bus 3. Figure 10 shows the plotting of eigenvalues with and without stabilizer connected at Bus 3. It can be observed that the plotting of eigenvalue is scattered for the system without stabilizer, while with stabilizer the plotting of eigenvalues is concentrating near to the imaginary axis.

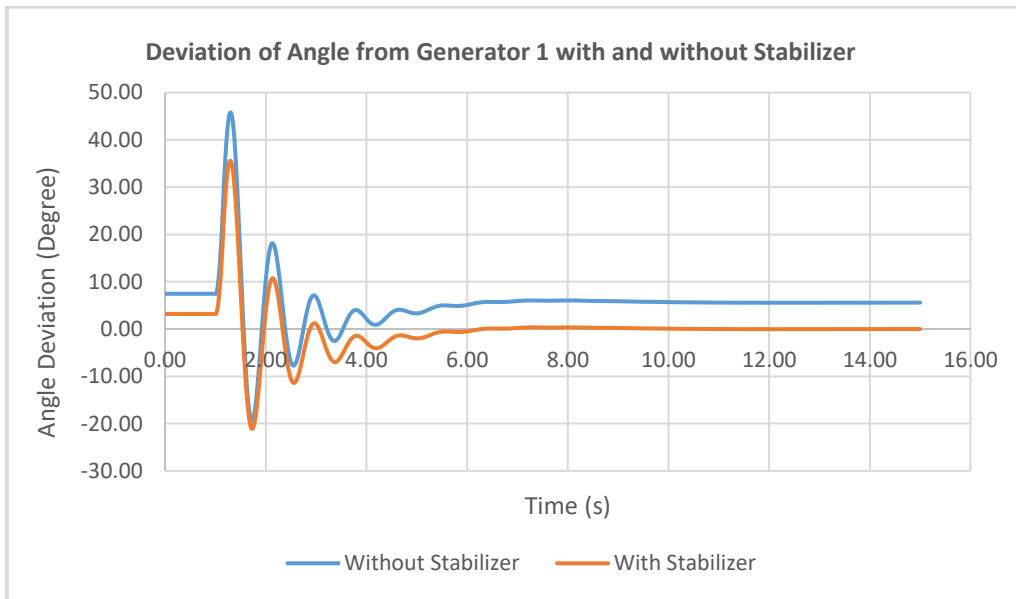


Figure 9: Rotor Angle at Bus 3

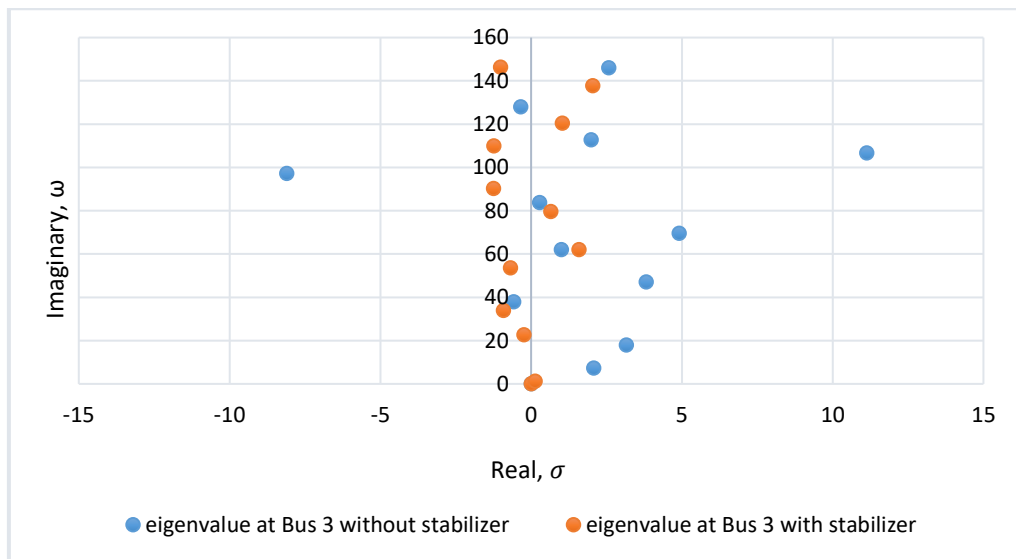


Figure 10: Location of Eigenvalue with and without Stabilizer

Figure 11 shows the accelerating power at Bus 3 with and without placing a stabilizer in the system. It can be seen that initially the accelerating power without stabilizer has higher peak values during both positive and negative cycles compared to the accelerating power with stabilizer. Higher accelerating power in the system without stabilizer leads to higher frequency oscillation as shown in Figure 12. This shows that the damping effect of the system with stabilizer is better than the system without stabilizer. Hence, a power system is more stable if it is connected with stabilizer.

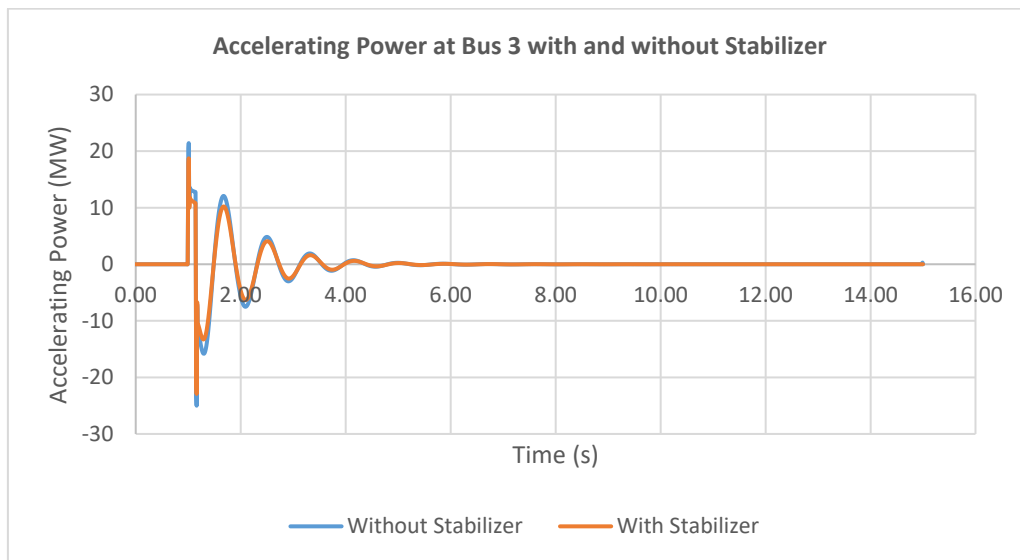


Figure 11: Accelerating Power at Bus 3 with and without Stabilizer

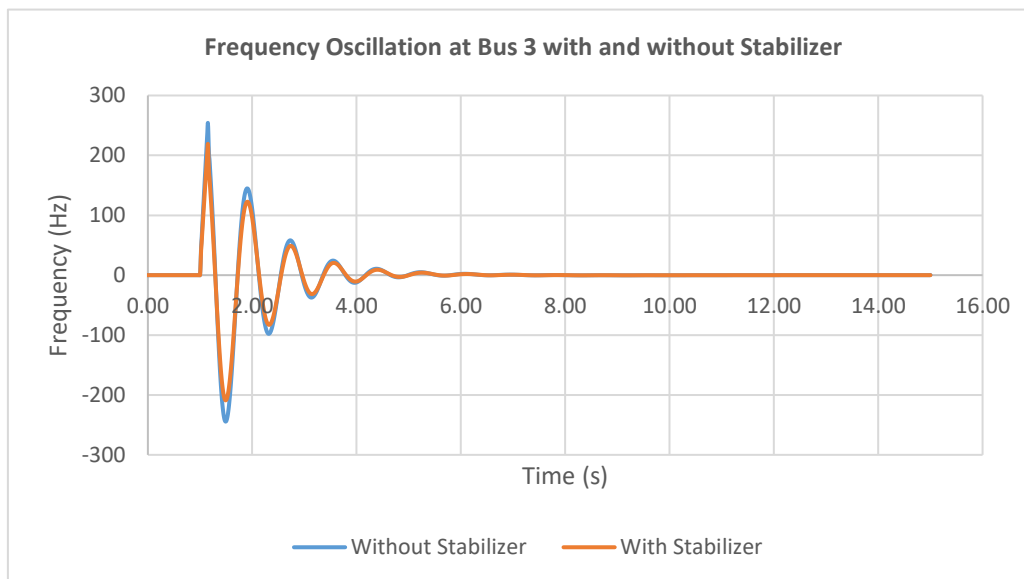


Figure 12: Frequency Oscillation at Bus 3 with and without Stabilizer

Case 3: Line fault between Bus 3 and Bus 4 with and without solar PV penetration at Bus 4

- **Without Solar PV Penetration**

The damping ratio is compared when line fault occurs between Bus 3 to Bus 4 with and without Solar PV penetration; Figure 13 shows the connection between Bus 3 and Bus 4. Power consumed by the apparent load at Bus 4 is $47.8 + j3.9$ MVA. The solar generation is connected to Bus 4 with generated power of 10 MW. This amount of Solar PV penetration is within the limit as regulated by the Energy Commission (EC), which states that for a Large Scale Solar (LSS) the minimum size of solar PV is 1MW and the maximum of 50MW could be connected to a substation [18].

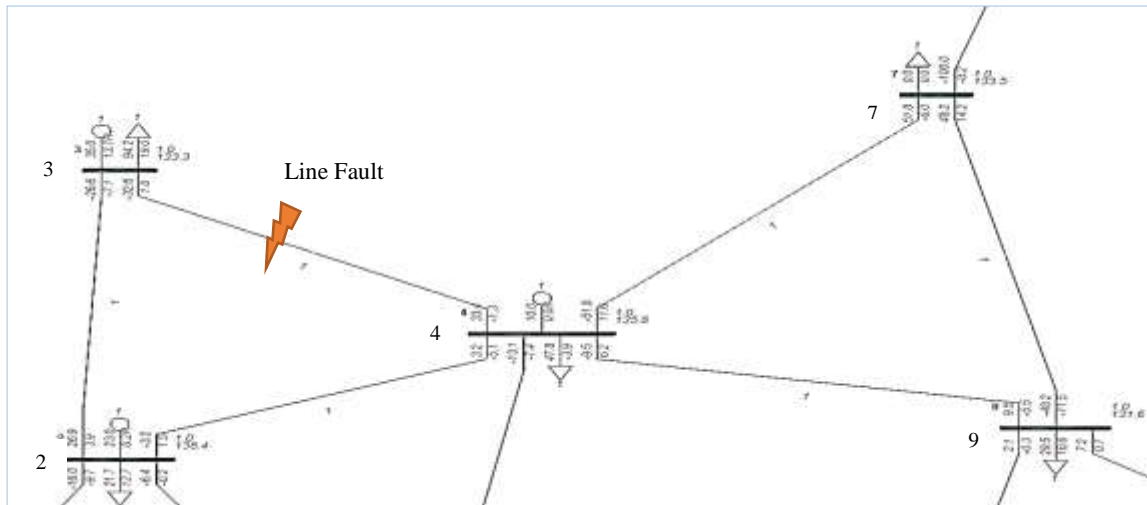


Figure 13: Network Connection between Bus 3 and Bus 4

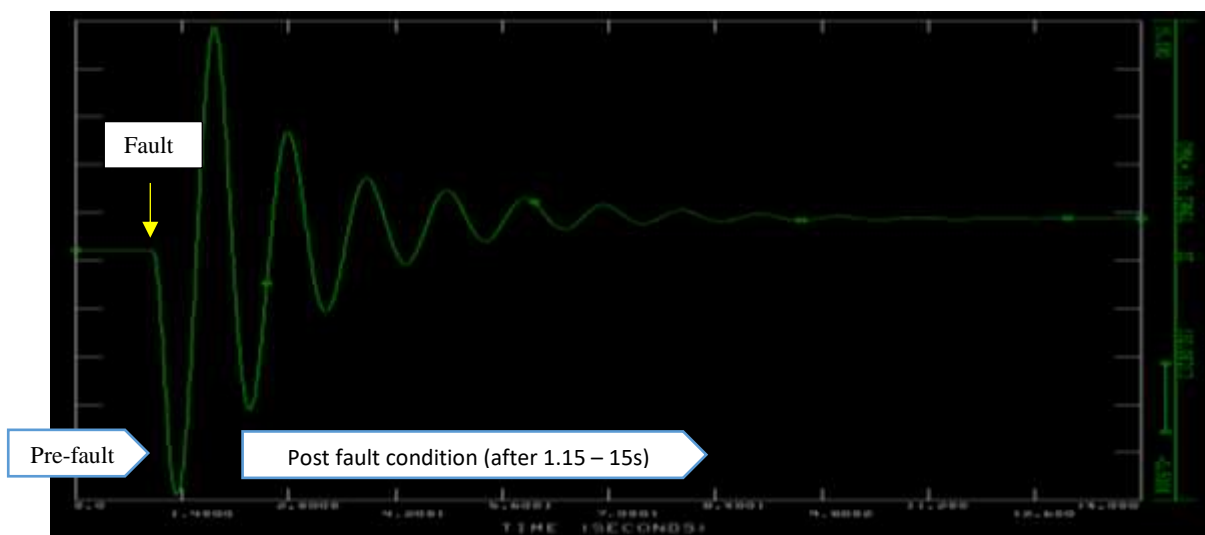


Figure 14: Rotor Angle Deviation at Bus 3 due to Line Fault between Bus 3 and Bus 4 without Solar PV Penetration

Figure 14 shows rotor angle deviation excursion at Bus 3 when line fault occurs between Bus 3 and Bus 4 without any solar PV penetration. The settling time for steady state condition is 11.2 seconds with rotor angle deviation of 10.9°. Based on the results, the eigenvalues being obtained using Prony Method through PSSPLT. The pole and zero values of each component of eigenvalues are analyzed to determine whether the locations of the poles and zeroes are within the stable region. It is clearly seen that the positive damping ratio has more than negative damping ratio. In addition, it is found that the frequency oscillation produced by each components are not classified in either local mode or inter-area mode, except for component 2 which has inter-area mode of 0.84 Hz. Those local mode and inter-area mode are of low frequency oscillation, which means that it has insufficient damping torque. The result of damping ratio for Bus 3 without connecting solar PV at Bus 4 is shown in Table 5. The damping ratio at component 3 is 0.098. The negative damping ratio is at component 2, 7, 11-12 and 14 and the positive damping ratio is at component 1, 3-6, 8-10 and 13 but of low values.

Table 5: Damping Ratio for Case 3 without Solar PV Penetration

Component	Eigenvalues		Real, σ	Imaginary, ω	Damping ratio, ξ	Frequency, Hz
	Real	Imaginary				
1	-0.1192E-03	-	-0.000119	0	1	sc
2	1.2313	5.2769	1.251	5.277	-0.231	0.840
3	-7.5912	76.9958	-7.591	76.996	0.098	12.254
4	-4.93112	24.4751	-4.931	24.475	0.198	3.895
5	-8.5987	57.4436	-8.599	57.444	0.148	9.142
6	-3.7592	79.9252	-3.759	79.925	0.047	12.720
7	0.4375	38.2065	0.438	38.207	-0.011	6.081
8	-1.7724	94.9163	-1.772	94.916	0.019	15.106
9	-7.5139	125.2100	-7.514	125.210	0.060	19.928
10	-7.1963	146.3080	-7.196	146.308	0.049	23.286
11	1.7864	108.6890	1.786	108.689	-0.016	17.298
12	6.9236	49.7805	6.924	49.781	-0.138	7.923
13	-0.8597	1542.538	-0.860	154.538	0.006	24.596
14	11.0701	125.831	11.070	125.831	-0.088	20.027

• **With Solar PV Penetration**

Line fault is exerted between Bus 3 and Bus 4, and solar generation is connected to Bus 4 generating 10 MW power. Figure 15 shows the damping effect to Generator 3 rotor angle at Bus 3 taking Generator 1 rotor angle at Bus 1 as reference, with and without solar PV connection of at Bus 4.

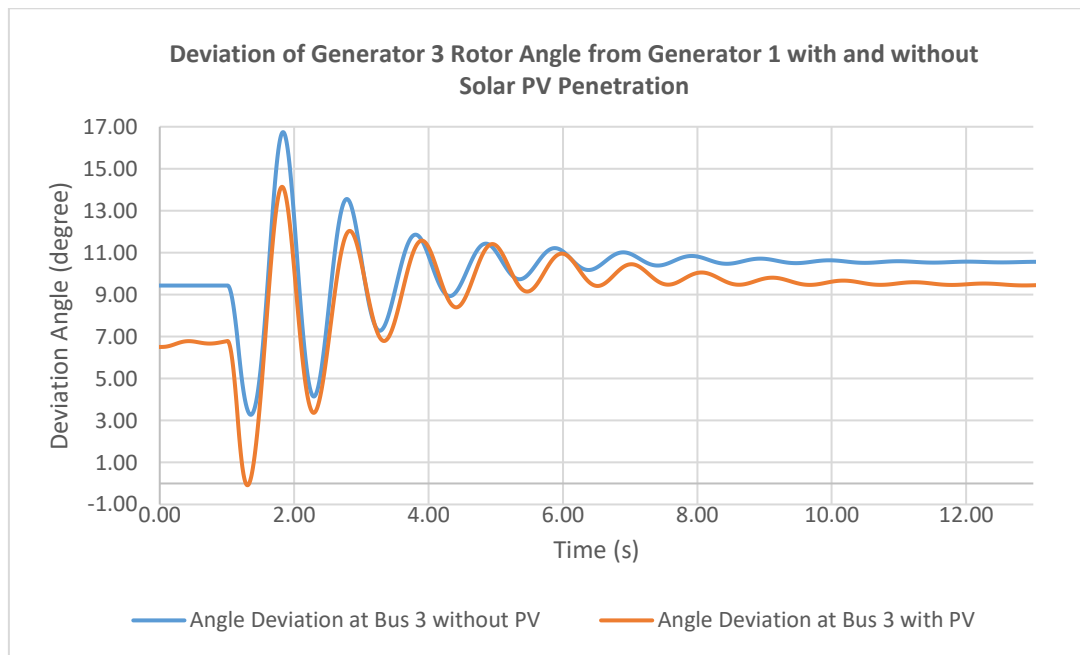


Figure 15: Deviation of Rotor Angle at Bus 3 from Reference Rotor Angle at Bus 1 with and without Solar PV Penetration at Bus 4

Referring to Figure 15, the maximum angle deviation at Bus 3 with solar PV connection to Bus 4 is 14.44°, while without solar PV connection the peak angle deviation is almost 17°. The damping of rotor angle for Bus 3 connected with solar PV shows better damping effect compared to without solar PV penetration. Nevertheless, for both cases, the settling time for the rotor angle to achieve steady state is approximately 11 seconds. The eigenvalues of rotor angle at Bus 3 with solar PV are obtained using modal analysis, Prony Method in PSSPLT as shown in Table 6. The damping ratio and respective frequency oscillation are calculated respectively. The frequency of the eigenvalues is not considered as Low Frequency Oscillation (LFO) except for component 2 and

3. Since the frequency for these two components are in the range between 1 to 2 Hz, therefore component 2 and 3 are under local mode where the oscillation occurs at small part of power system.

Table 6: Damping Ratio for Case 3 with Solar PV Penetration

Component	Eigenvalues		Real, σ	Imaginary, ω	Damping ratio, ξ	Frequency, Hz
	Real	Imaginary				
1	0.1969E-01	-	0.0197	0	-1	0
2	-1.0939	8.8937	-1.093	8.893	0.122	1.415
3	-26.4377	9.9892	-26.438	9.990	0.935	1.590
4	-1.0114	14.3574	-1.011	14.357	0.070	2.285
5	6.6373	-	6.637	0	-1	0
6	-17.3929	39.0508	-17.393	39.051	0.407	6.215
7	-1.1289	52.2933	-1.129	52.293	0.022	8.323
8	-1.6088	115.2000	-1.609	115.200	0.014	18.335
9	-0.84312	127.7250	-0.843	127.725	0.007	20.328
10	-2.8605	144/3570	-2.860	144.357	0.020	22.975
11	-1.5471	77.2669	-1.547	77.267	0.020	12.297
12	1.9507	154.580	1.951	154.580	-0.013	24.602
13	7.0177	66.0407	7.018	66.041	-0.106	10.511
14	1.7815	92.0477	1.781	92.048	-0.019	14.650

The system is said to be at unstable condition if the damping ratio, ξ is negative [13]. With solar PV penetration, the damping ratio of component 3 has increased to 0.935 from 0.098 for without solar PV, an increment of about 0.837. The damping ratio is positive at component 2 - 4 and 6 - 11 while negative damping ratio for component 1, 5, and 12-14; thus, majority of the damping ratio is positive. The critical eigenvalue at component 2 gives a better result performance when solar PV is connected to Bus 4 which has an increase in damping ratio from -0.231 to 0.122. Besides that, when the grid is connected with solar energy, the stability can be increased to 11% margin [2]. The damping ratio for cases with PV has improved from 9.81% to 93.545%. Thus, the stability of the system is improved.

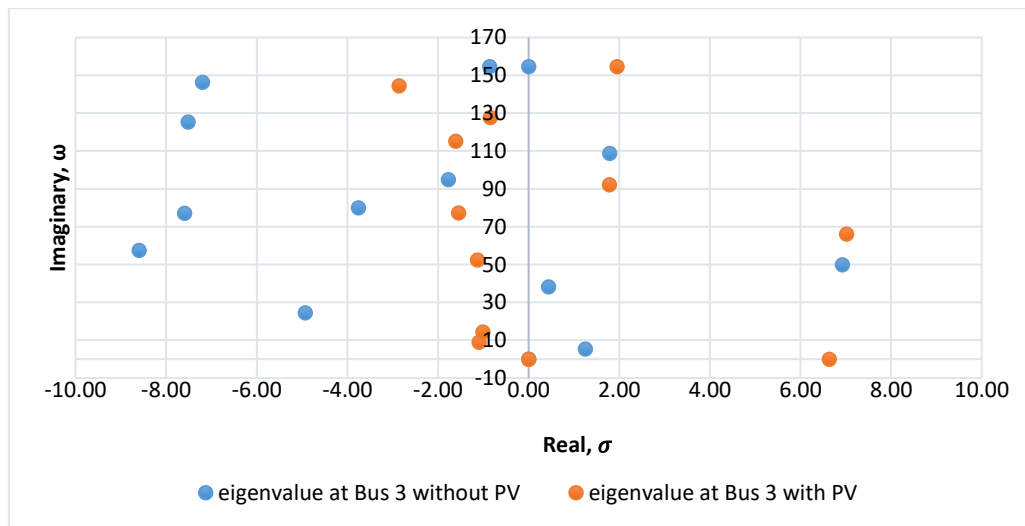


Figure 16: Location of Eigenvalue with and without Solar PV Penetration

Figure 16 shows the location eigenvalue with and without solar PV penetration. The locations of eigenvalue for system without solar PV connection are scattered, while with solar PV penetration the eigenvalues locations move near to the imaginary axis; thus, the system becomes more stable. Figure 17 shows Bus 3 accelerating power when the system is with and without solar PV injection. The accelerating power of the system with solar PV penetration is higher compared to the system without solar PV; however, the period of each oscillation elongates as it moves towards the same settling time.

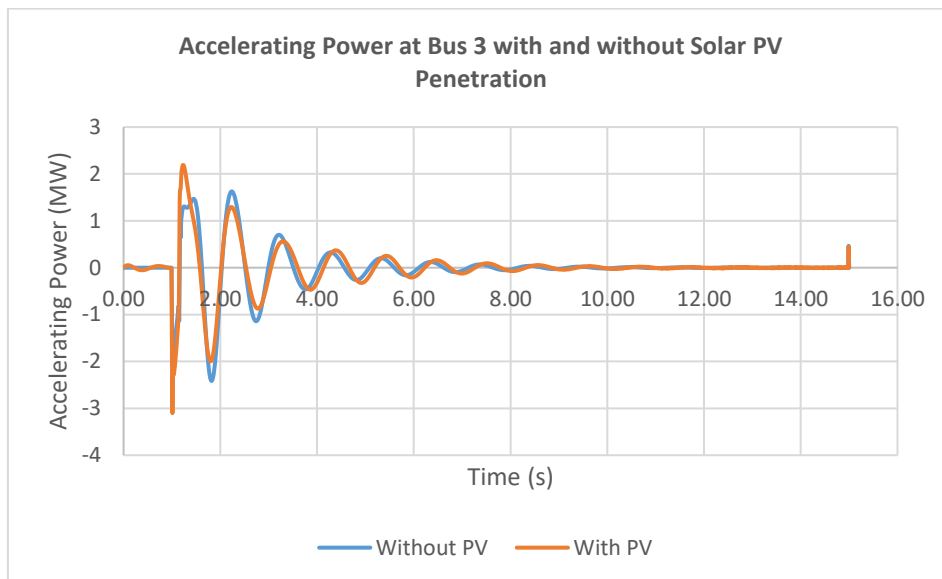


Figure 17: Accelerating Power at Bus 3 with and without Solar PV Penetration

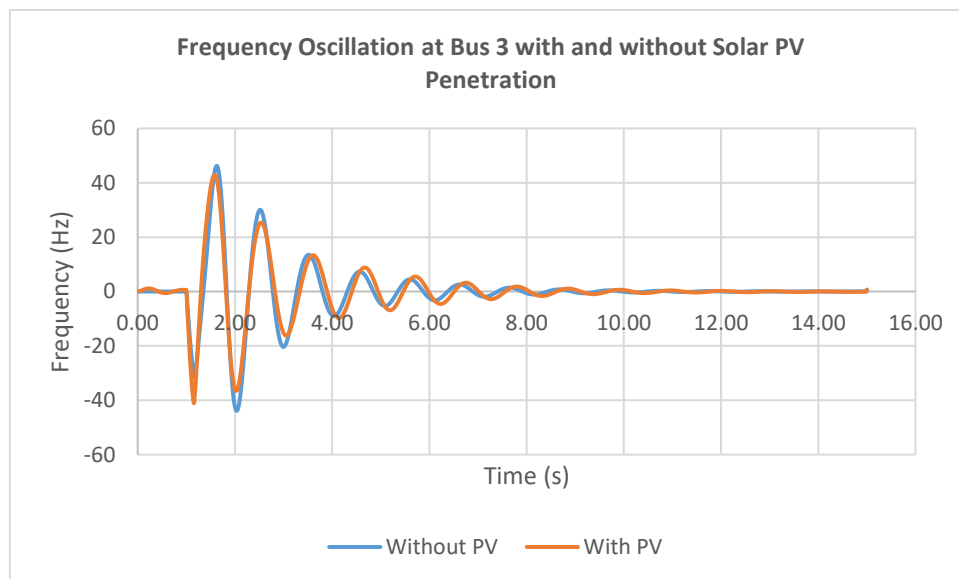


Figure 18: Frequency Oscillation at Bus 3 with and without Solar PV Penetration

Figure 18 shows the frequency oscillation at Bus 3 with and without the presence of solar PV in the system. The frequency of oscillation is consistent with the accelerating power as it moves towards the same settling time.

IV. CONCLUSION

Research work has demonstrated that in analyzing small signal stability of a power system, the findings obtained using accelerating power, oscillation frequency, eigenvalues, and damping ratio complement each other. Furthermore, the plotting of the accelerating power enables the researcher to determine the settling time for a power system to reach its steady state condition after subjected to disturbance. In addition, it is proven that power system stabilizer helps a power system to reach its state of stability faster after the occurrence of fault. Furthermore, it has been proven that solar PV penetration can increase the stability of the system by increasing

the damping ratio. As a conclusion, analysis on the impact of renewable energy penetration in power system network to small signal stability is important in determining whether the system could maintain its stability and reliability when subjected to disturbance.

V. ACKNOWLEDGEMENTS

The research team would like to acknowledge the Ministry of Higher Education (MOHE) for the research funding (20140135FRGS) on 'Optimum renewable energy penetration using Wide Area Intelligent System with consideration towards line loadability, protective relaying performance and self-healing adaptation in maintaining power system stability'. The team would also like to extend acknowledgments to Universiti Tenaga Nasional, Tenaga Nasional Berhad and lecturers for providing the facilities and making this research possible.

REFERENCES

- [1] S. Chopde and S. Patil, "Influence of grid connected solar and wind energy on small signal stability," in *Advancements in Power and Energy (TAP Energy), 2015 International Conference on*, 2015. R.
- [2] Krishan, A. Verma and B.Prasad, "Small Signal Stability and Analysis of Grid Connected Distributed PV and Wind Energy System," *IEEE*, 2014.
- [3] SEDA, "NEM Concept," Sustainable Energy Development Authority Malaysia, 2017. [Online]. Available: <http://seda.gov.my/>. [Accessed 10 August 2017].
- [4] P. Kundur, J. Paserba and S. Vitet, "Overview on definition and classification of power system stability," *IEEE/CIGRE Joint Task Force on Stabilia Terms and Definitions*, pp. 1-15, 2003.
- [5] H. U. Banna, A. Luna, S. Ying, H. Ghorbani and P. Rodriguez, "Impacts of Wind Energy In-Feed on Power System Small Signal Stability," in *3rd International Conference on Renewable Energy Research and Applications*, Milwaukee, USA, 2014.
- [6] R. W. Jr, "Identification of Power System Stability Using Relevant Modes," University of New Orleans, New Orleans, 2011.
- [7] I. I. Hamarash, "Small Signal Stability Analysis of Kurdistan Regional Power System," in *Research Gate*, 2012.
- [8] P. Kundur, *Power System Stability And Control*, United State : McGraw-Hill, 1994.
- [9] . H. Liu, L. Jin, D. Le and A. A. Chowdhury, "Impact of High Penetration of Solar Photovoltaic Generation on Power System Small Signal Stability," in *International Conference on Power System Technology*, 2010
- [10] D. o. M. Engineering, "Understanding Poles and Zeros," Massachusetts Institute of Technology
- [11] E. P. R. De and M. Ques, "Analysis and Damping of Inter-Area Oscillation in the UCTE/CENTREL Power System," *Session 2000 at CIGRE*, pp. 1-10, 2000.
- [12] Transmission System Reliability Standards, Tenaga Nasional Berhad (TNB), Version 2, Edition 1, 2006
- [13] L. Yun, D. Liu and R. Wang, "Influencing Factors Analysis of Damping Characteristics on Low Frequency Oscillation," in *Proceedings of the 2011 International Conference on Power Engineering, Energy and Electrical Drives*, Torremolinos (Málaga), Spain, 2011.
- [14] K. Prasertwong, M. Nadarajah and D. Thakur, "Understanding Low Frequency Oscillation in Power Systems," *International Journal of Electrical Engineering Education*, pp. 1-12, 2010.
- [15] Program Application Guide Volume 2, Siemens Industry, Inc., Siemens Power Technologies International, Schenectady, NY, pp. 519-521, 2016.
- [16] S. M. Shahruz, G. Langari and M. Tomizuka, "Optimal damping ratio for linear second-order systems," *Journal of Optimization Theory and Applications*, vol. 73, no. 3, pp. 563-576, 1992.
- [17] P. Pavan Kumar, M. Ravindra Babu and G. Saraswathi, "Dynamic analysis of single machine infinite bus system using single input and dual input PSS," *Electrical Engineering*, vol. 13, no. 1, pp. 72-81, 2013.
- [18] S. Tenaga, *Guidelines on Large Scale Solar Photovoltaic Plant for Connection to Electricity Networks*, Malaysia: Suruhanjaya Tenaga, 2016.

CITE AN ARTICLE

Zaman, N. K., Yusoff, M. E., & Hashim, H. (2018). ANALYSIS ON THE IMPACT OF POWER SYSTEM STABILIZER AND RENEWABLE ENERGY TO SMALL SIGNAL STABILITY OF A POWER SYSTEM. INTERNATIONAL JOURNAL OF ENGINEERING SCIENCES & RESEARCH TECHNOLOGY, 7(8), 477-492.